Structural Eng./Earthquake Eng., JSCE, Vol.22, No. 1, 15s-26s, 2005 April
(J. Struct. Mech. Earthquake Eng., JSCE, No.787/I-71)

DEVELOPMENT OF A REGIONAL MAP OF EXTREME WIND SPEEDS IN THE PHILIPPINES

Lessandro Estelito GARCIANO[1], Masaru HOSHIYA[2] and Osamu MARUYAMA[3]

[1]Student Member, JSCE, Graduate Student, Dept. of Civil Eng., Musashi Institute of Technology
(1-28-1 Tamazutsumi, Setagaya-ku, Tokyo 158-8557, Japan)
E-mail: g0265018@sc.musashi-tech.ac.jp
[2]Member, JSCE, Professor, Dept. of Civil Eng., Musashi Institute of Technology
(1-28-1 Tamazutsumi, Setagaya-ku, Tokyo 158-8557, Japan)
E-mail: mhoshiya@sc.musashi-tech.ac.jp
[3]Member, JSCE, Asst. Professor, Dept. of Civil Eng., Musashi Institute of Technology
(1-28-1 Tamazutsumi, Setagaya-ku, Tokyo 158-8557, Japan)
E-mail:omaruya@sc.musashi-tech.ac.jp

This paper presents an improvement of the current wind zone map of the Philippines. The Generalized Extreme Value (GEV), Gumbel and point process models were used in characterizing the extreme wind speeds in the Philippines. Available daily maximum wind data from 50 stations in the Philippines were also used in the analysis. The results show that the standard errors in the point process model are lower than the GEV or Gumbel models making it a better model. Finally a regional wind zone map (6 zones) was developed using extrapolated 30, 40 and 50 year return wind speeds from the point process approach. Wind zone maps were developed using kriging interpolation method of ArcGIS Geostatistical Analyst.

Key Words : *GEV, point process, kriging, extreme wind speeds, wind zone map*

1. INTRODUCTION

The Philippines is prone to natural hazards like earthquakes and typhoons. An average of twenty typhoons enter into Philippine Areas of Responsibility each year. These typhoons which bring about strong winds and heavy rainfall cause heavy damage to life and property. It is for this reason that a wind zone map is important. It helps planners assess the levels of extreme wind speeds in the future and hence design safe and reliable structures.

The National Structural Code of the Philippines (NSCP)[1)] , adopted a recommendation published by the Association of Structural Engineers of the Philippines (ASEP), to divide the country into three wind zones, as shown in **Fig. 1**. Corresponding to these zones are basic wind speeds V, which when multiplied with other factors will result in a velocity pressure for structural design purposes. In recent years, there has been a development in the statistical

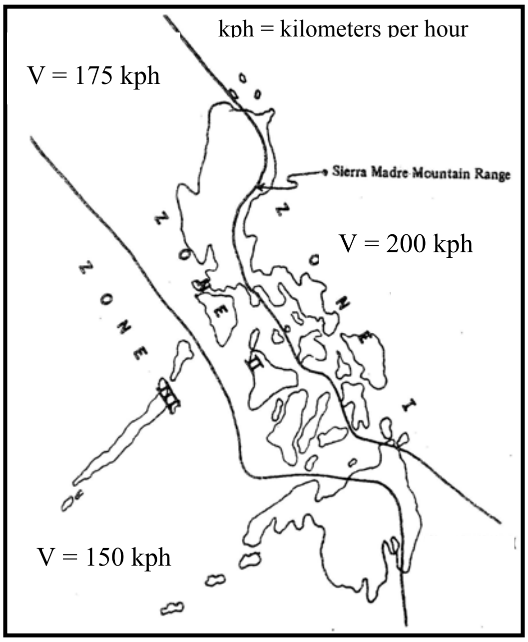

Fig. 1 NSCP (1992) Wind Zone Map

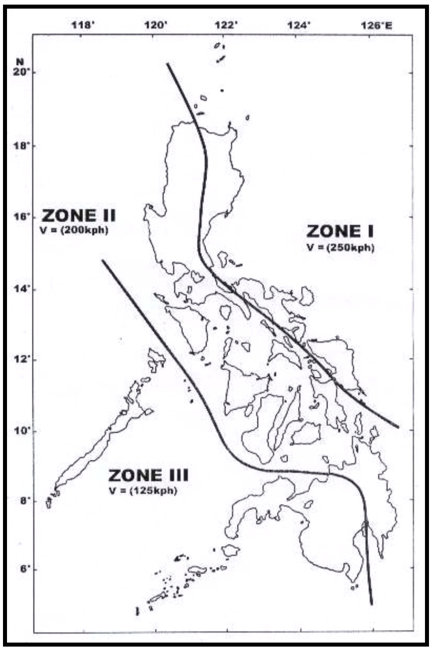

Fig. 2 NSCP (2001) Wind Zone Map

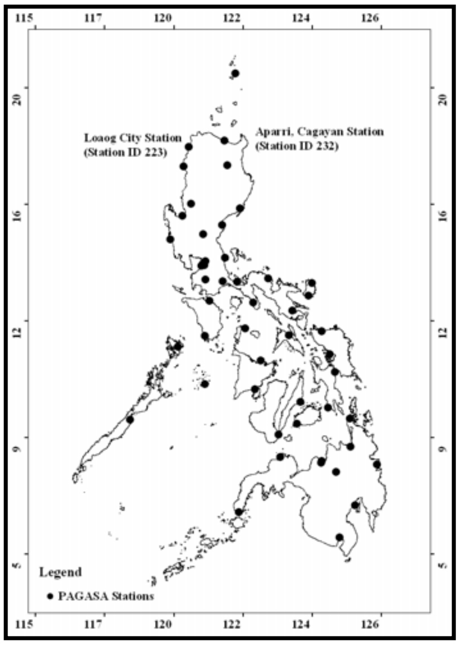

Fig. 3 Location of PAGASA Weather Stations

treatment of extreme events; Coles & Pericchi[2], Ferreira & Guades Soares[3], Smith[4], wind zone mapping; Peterka & Shahid[5] and the wind code provisions[6].

In view of this, ASEP updated the NSCP wind code to adapt to these changes. The wind zone map was also updated for this purpose as shown in **Fig. 2**. This map was adopted in part from Rosaria[7]. The changes that are evident in the recent map are primarily due to the modeling technique used. The Type I (Gumbel) model was used to obtain the basic wind speeds. This map was also developed using 35 years (1961 to 1995) of monthly maximum data from 50 weather stations of the Philippine Atmospheric, Geophysical and Astronomical Services (PAGASA).

In this paper, we select the most appropriate extreme value model, e.g. GEV or point process approach to model the extreme wind speeds in the Philippines. Recent and daily maximum wind data are also used in the analysis to improve the accuracy in the inference. The main objective of this paper is to develop a regional wind zone map of extreme wind speeds in the Philippines with return periods of 30, 40 and 50 years.

2. THE DATA

The wind data used in this paper were taken from the 50 weather stations of PAGASA. The locations of the stations are shown in **Fig. 3**. Wind speeds were measured by anemometers from a height of 10 meters above the ground. PAGASA records two kinds of data, daily average wind speed and maximum wind speed both in m/s. According to PAGASA, only wind speeds reaching 8 m/s and above are recorded as maximum wind speed.

In this paper we only consider these maximum wind speeds. It is assumed that the wind data are meteorologically homogenous and nominally consist of the following:

1. 35 years (1961 to 1995) of monthly maximum wind speeds from the 5 stations.
2. 40 years (1961 to 2000) of daily maximum wind speeds (> 8 m/s) from 45 stations.

Some wind data exceeding 70 m/s were found and were corrected by PAGASA. Data were also missing at random from the different stations due to various sources and the stations did not operate simultaneously from 1961. Characteristics like the mean and standard deviation of the maximum wind speeds for each station are shown in **Fig. 4**. Likewise a summary of the available data used in this study is shown in **Table 1**.

3. EXTREME VALUE MODELS

(1) GEV Distribution[8]

Suppose we have a sequence of independent random variables $X_1, ..., X_n$ with a common distribution function F. One way of characterizing the behaviour of extremes is by considering the behavior of $M_n = \max(X_1, ..., X_n)$, given by the nth power of F.

Table 1 PAGASA weather stations description

Station No. and Name	Station ID	Lati-tude	Longitude	Elevation, in m	Data Period, in Years	Remarks/ Missing Years
1 Alabat, Quezon	435	14.02	122.02	5.0	1961 - 2000	
2 Ambulong, Batangas	432	14.08	121.05	10.0	1964 - 2000	
3 Aparri, Cagayan	232	18.36	121.63	0.3	1961 - 2000	
4 Baguio City, Benguet	328	16.42	120.60	1500.0	1961 - 2000	
5 Baler, Quezon	333	15.77	121.57		1961 – 1994	
6 Basco, Batanes	135	20.45	121.96	11.0	1961 – 2000	
7 Butuan City, Agusan del Norte	752	8.93	125.52	17.7	1981 – 2000	
8 Cabanatuan, Nueva Ecija	330	15.48	120.97		1961 – 1995	Mo. maximum only / 1962 - 1964
9 Cagayan de Oro, Misamis Oriental	748	8.48	124.63	6.0	1961 - 2000	1962 to 1964, 1966
10 Calapan, Oriental Mindoro	431	13.42	121.18	40.5	1961 - 2000	
11 Casiguran, Quezon	336	16.28	122.12	4.0	1961 - 2000	
12 Catarman, Northern Samar	546	12.50	124.63	5.0	1961 - 2000	
13 Catbalogan, Western Samar	548	11.78	124.88	5.0	1961 - 2000	
14 Coron, Palawan	526	12.00	120.20	14.0	1962 - 2000	1963
15 Cuyo, Palawan	630	10.85	121.03	4.0	1961 - 2000	1991
16 Daet, Camarines Norte	440	14.12	122.98	4.0	1961 - 2000	
17 Dagupan City, Pangasinan	325	16.05	120.33	2.0	1961 - 2000	
18 Davao City, Davao del Sur	753	7.12	125.65	18.0	1961 - 2000	
19 Dipolog, Zamboanga del Norte	741	8.60	123.35	4.0	1961 - 2000	1962 and 1963
20 Dumaguete City, Negros Oriental	642	9.30	123.30	8.0	1961 - 2000	1962
21 General Santos, South Cotabato	851	6.12	125.18	15.0	1964 - 2000	
22 Hinatuan, Surigao del Sur	755	8.37	126.33	3.0	1962 - 2000	1963, 1966 – 1968
23 Iba, Zambales	324	15.33	119.97	4.7	1961 - 2000	1962
24 Iloilo City, Iloilo	637	10.70	122.57	8.0	1961 - 2000	
25 Infanta, Quezon	434	14.75	121.65	7.0	1961 - 2000	
26 Laoag City, Ilocos Norte	223	18.18	120.53	5.0	1961 - 2000	
27 Legaspi City, Albay	444	13.13	123.73	17.0	1961 - 2000	
28 Lumbia Airport, Misamis Oriental	747	8.43	124.62		1977 – 1995	Mo. maximum only / 1991
29 Maasin, Southern Letyte	648	10.13	124.83		1972 – 1995	Monthly maximum only
30 Mactan International Airport	646	10.30	123.97	12.8	1972 – 2000	
31 Malaybalay, Bukidnon	751	8.15	125.08	627.0	1962 – 2000	1997
32 Masbate, Masbate	543	12.37	123.62	6.0	1961 – 2000	
33 NAIA (MIA), Pasay City	429	14.52	121.02	21.0	1961 – 2000	
34 Port Area (MCO), Manila	425	14.58	120.98	16.0	1961 – 2000	1980
35 Puerto Princesa, Palawan	618	9.75	118.73	16.0	1961 – 2000	
36 Romblon, Romblon	536	12.58	122.27	47.0	1961 – 2000	1984
37 Roxas City, Aklan	538	11.58	122.75	4.0	1961 – 2000	1962 to 1963
38 San Francisco, Quezon	437	13.37	122.52		1966 – 1995	Mo. max. only / 1978-1985,1987-1991
39 San Jose, Occidental Mindoro	531	12.35	121.03	0.3	1981 - 2000	
40 Sangley Point, Cavite	428	14.50	120.92	3.0	1974 - 2000	
41 Science Garden, Quezon City	430	14.65	121.05	43.0	1961 – 2000	
42 Surigao, Surigao del Norte	653	9.79	125.492	39.0	1961 – 1995	Mo. max. only / 1964, 1979 to 1983
43 Tacloban City, Leyte	550	11.23	125.03	3.0	1961 - 2000	
44 Tagbilaran City, Bohol	644	9.63	123.87	6.0	1961 - 2000	
45 Tayabas, Quezon	427	14.03	121.58	157.7	1971 - 2000	
46 Tuguegarao, Cagayan	233	17.62	121.73	61.6	1961 - 2000	
47 Vigan, Ilocos Sur	222	17.56	120.38	33.0	1961 - 2000	
48 Virac Radar, Catanduanes	447	13.61	124.30	233.0	1968 - 2000	
49 Virac Synop, Catanduanes	446	13.58	124.23	40.0	1961 - 2000	
50 Zamboanga City, Zambo.del Sur	836	6.90	122.07	6.0	1961 - 2000	

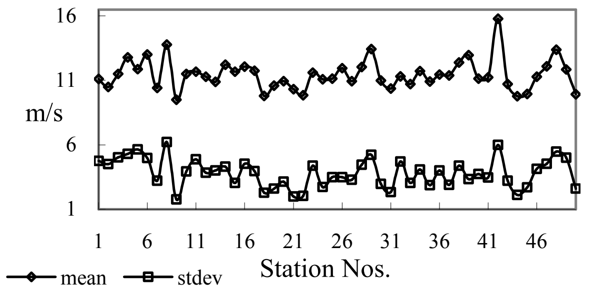

Fig .4 Mean and standard deviation of gusts for each station

$$P(M_n \le z) = P(X_1 \le z, ..., X_n \le z) = P(X_1 \le z) \cdot ... \cdot P(X_n \le z) = \{F(z)\}^n \quad (1)$$

Since F can be estimated from observed data, it is possible to use this in Eq. (1), but slight inaccuracies in estimating F lead to considerable error in F^n. However, if M_n can be stabilized by a linear re-normalization by defining $M_n^* = (M_n - a_n)/b_n$, where $a_n > 0$ and b_n as sequences of constants, then M_n^* has a limiting distribution known as the GEV with distribution:

$$G(x; \mu, \sigma, \xi) = \exp(-[1 + \xi(x - \mu)/\sigma]^{-1/\xi}) \quad (2)$$

The parameters μ, $\sigma(>0)$ and ξ are referred to as the location, scale and shape parameters respectively. The parameterization of the original three family Extreme Value Distribution are obtained by:

1. Taking the limit of Eq. (2) as $\xi \to 0$ recovers the Type I (Gumbel) distribution with

$$G(x; \mu, \sigma)_{\xi \to 0} = \exp(-\exp(-(x - \mu)/b)) \quad (3)$$

2. Setting $\xi = 1/\alpha > 0$, $\sigma = b/\alpha > 0$ and $\mu = a + b$ recovers the Type II (Fréchet) distribution with $\xi > 0$,
3. Setting $\xi = -1/\alpha < 0$, $\sigma = b/\alpha > 0$, and $\mu = a + b$ recovers the Type III (reversed Weibull) distribution with $\xi < 0$.

There are several methods in the inference of extreme value models and in this paper we will use the maximum likelihood estimate (MLE). The preference for this method is it possess several desirable properties, e.g., simplicity in maximing the log-likelihood function, standard errors and confidence intervals can be approximated, minimum variance for large sample size, can be used to test the null hypothesis that the GEV model can be reduced to Gumbel model using the likelihood ratio test.

To obtain estimates of extreme quantiles of the annual maximum distribution the following equations are used:

$$x_p = \begin{cases} \mu - \sigma[1 - \{-\log(1-p)\}^{-\xi}]/\xi & \text{for } \xi \ne 0 \\ \mu - \sigma \log\{-\log(1-p)\}, & \text{for } \xi = 0 \end{cases} \quad (4)$$

where $G(x_p) = 1 - p$. In extreme value terminology, x_p is the return level associated with the return period $1/p$. In particular, x_p is exceeded by the annual maximum in any particular year with probability p. The 95% confidence intervals (CI) for x_p are obtained by using the delta method and the observed information matrix.

To test the null hypothesis that the GEV model can be reduced to Gumbel model we make use of the likelihood ratio test. For example, define the likelihood ratio statistic or also known as the deviance statistic

$$D = 2[\ell_{GEV}(\hat{\theta}^{(1)}) - \ell_{Gum}(\hat{\theta}^{(0)})] \quad (5)$$

where ℓ_{GEV} and ℓ_{Gum} are the maximimized likelihoods for the GEV and Gumbel models with respective MLEs $\hat{\theta}^{(1)}$ and $\hat{\theta}^{(0)}$. If the Gumbel model is a valid model then, approximately, $D \sim \chi_1^2$, the chi-squared distribution with one degree of freedom. Thus, we reject the Gumbel model in favor of the GEV at significance level α if D is greater than the upper-α point of the χ_1^2.

(2) Modeling annual wind maxima

To apply GEV modeling, we will analyze time series of annual maximum wind speeds from two stations, specifically, the data sets from Aparri, Cagayan and Laoag City as shown in **Figs. 5** and **6**, respectively. The S-PLUS functions of Coles[9] are used to analyse these data sets as well as the wind data from the other stations.

The MLEs of the parameters of the wind data from Aparri, Cagayan station are $\hat{\mu}$ = 25.42, $\hat{\sigma}$ = 9.76 and $\hat{\xi}$ = 0.22. Substituting these MLEs into Eq. (4) gives a maximized negative log-likelihood (nllh) value of 159.27. Subsequently the standard errors and the approximate 95% CI of each parameters are

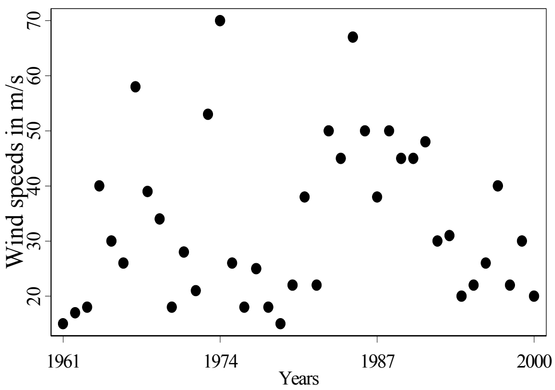

Fig. 5 Annual Maximum Wind Speeds at Aparri, Cagayan

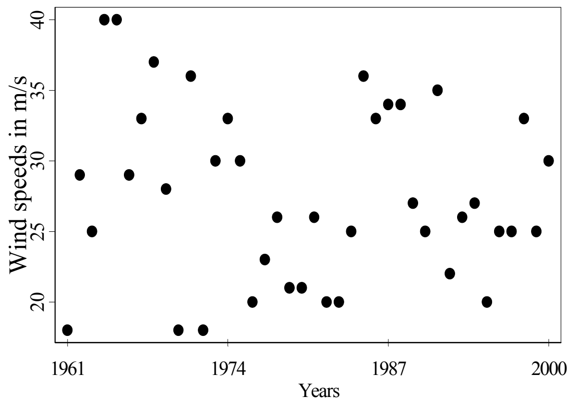

Fig. 6 Annual Maximum Wind Speeds at Laoag Station

calculated. The standard errors are $\hat{\mu}$ = 1.99, $\hat{\sigma}$ = 1.65 and $\hat{\xi}$ = 0.22 and the approximate 95% CI are [21.52, 29.32] for μ, [6.53, 12.99] for σ and [-0.21, 0.65] for ξ. Since the basic wind speeds in the recent wind zone map are associated with an annual probability of 0.02 of being equaled or exceeded, we follow this specification and therefore estimate the 50-year return wind speed.

The return wind speeds and CI are estimated by substituting the MLEs into Eq. (4) and setting p = 0.02. Therefore x_p = 85 m/s with variance, $\mathrm{var}(x_{0.02})$ = 664. The 95% CI for $x_{0.02}$ is $85 \pm 1.96\sqrt{664}$ = [34.85, 135.85]. **Fig. 7** is the return wind speed plot for Aparri, Cagayan station.

The MLEs of the parameters of the wind data from Laoag station are $\hat{\mu}$ = 25.21, $\hat{\sigma}$ = 5.75 and $\hat{\xi}$ = -0.21 with a nllh of 128.64. The standard errors are $\hat{\mu}$ = 1.07, $\hat{\sigma}$ = 0.80 and $\hat{\xi}$ = 0.16 and the approximate 95% CI are [23.11, 27.31] for μ, [4.18, 7.32] for σ and [-0.52, 0.65] for ξ. Setting $p = 0.02$ we obtain x_p = 40 m/s and with $\mathrm{var}(x_{0.02})$ = 8.01.

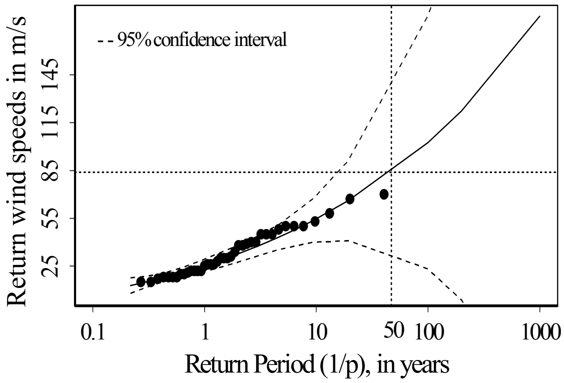

Fig .7 Return wind speeds for Aparri, Cagayan Station

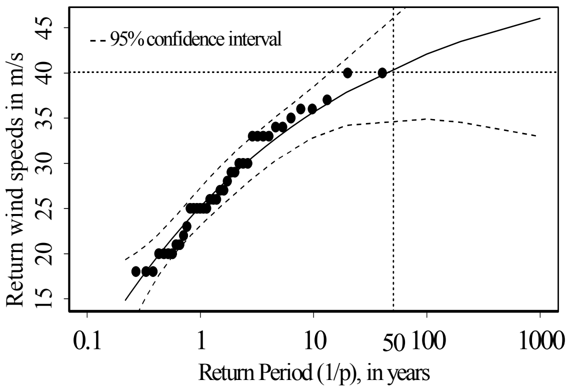

Fig. 8 Return wind speeds for Laoag Station

The estimated CI for $x_{0.02}$ is $40 \pm 1.96\sqrt{8.01}$ = [34.91, 46.00]. **Fig. 8** shows the return wind speed plot for Laoag station.

We can see from the preceding figures how the return wind speeds are influenced by the shape parameter. For Aparri, Cagayan with ξ > 0, the graph is concave with no finite bound and for Laoag with ξ < 0 it is convex with an asymptotic limit of $\mu - \sigma / \xi$ as $p \to 0$. The parameter ξ is a site-independent parameter and this paper does not attempt to correlate the values of ξ for both stations.

Since the recent wind zone map was basically derived from a Gumbel model, we test the null hypothesis of reducing the GEV model to a Gumbel model $(\xi = 0)$. The MLEs of the Gumbel parameters $(\hat{\mu}, \hat{\sigma})$ for Aparri, Cagayan and Laoag stations are (26.63, 10.89) and (24.59, 5.34) respectively. Substituting these MLEs into Eq. (4) gives a nllh value of 159.82 and 129.40. Therefore the D for Aparri and Laoag stations are 1.1 and 1.5 respectively which are small compared to the χ_1^2 distribution with 95% CI. Hence the Gumbel model is a probable model for these data.

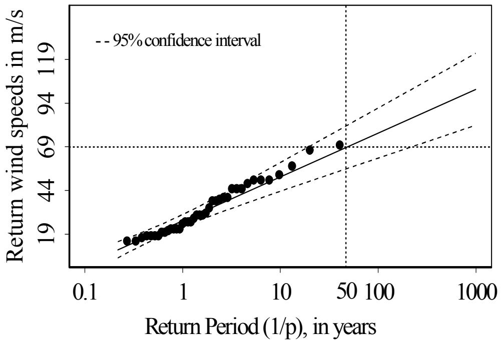

Fig. 9 Return wind speeds for Aparri, Cagayan Station

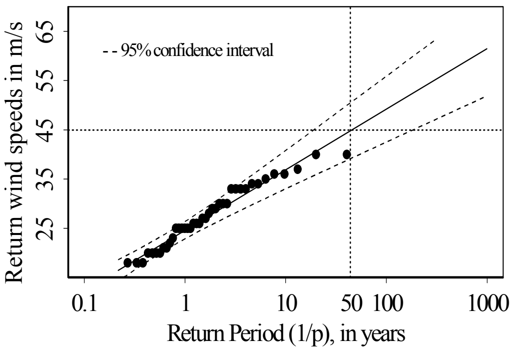

Fig. 10 Return wind speeds for Laoag City Station

The return level plots of the Gumbel model shown in **Figs. 9** and **10** also show that the goodness-of-fit is comparable to the GEV model. The rest of the data sets were also fitted to the GEV and Gumbel models.

The MLEs of the parameters μ and σ for each station are plotted in **Figs. 11** and **12**. The results of the MLEs of ξ will be shown later. The figures above show that for each station, the parameters μ and σ are similar in both models. We then reduce the GEV model to the simpler Gumbel model with only two parameters by computing the D for each station and comparing it with the χ_1^2 distribution. From **Fig. 13** we can see that the D from the 38 stations are small compared to the χ_1^2 distribution with 95% CI giving strong support in reducing the GEV model to a Gumbel model for these 38 stations.

However, if we examine carefully the parameter ξ of the GEV distribution for each station (**Fig. 14**), we can see that there are only 6 stations with $\xi \approx 0$ (Gumbel). Furthermore, there are 28 stations where $\xi > 0$ (Fréchet) and 16 stations where $\xi < 0$ (reversed weibull). This means that if we extrapolate return wind speeds, especially at high levels, overestimation and underestimation of wind speeds will occur. These happen because ξ influences the return wind speeds as mentioned earlier.

The preceding results show that both the GEV and

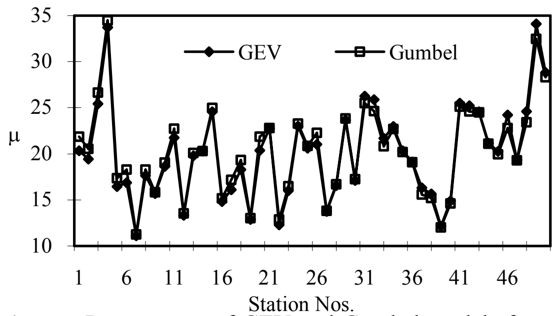

Fig. 11 Parameter μ of GEV and Gumbel models for each station

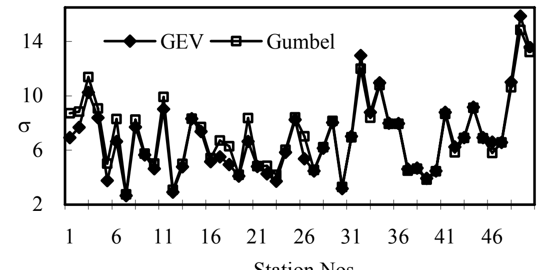

Fig. 12 Parameter σ of GEV and Gumbel models for each station

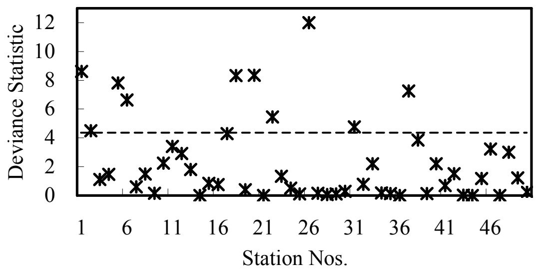

Fig .13 Deviance Statistic D for each station

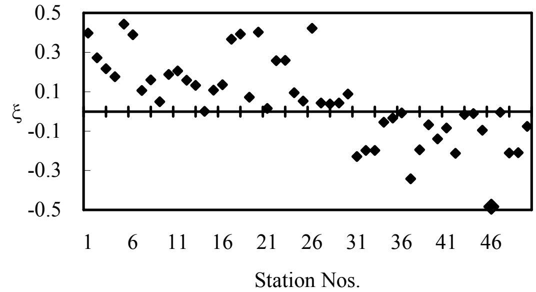

Fig .14 Parameter ξ of GEV model for all stations

the Gumbel models are suitable exteme value models for annual wind speed maxima. However the point of the analysis is to establish design parameters (extreme wind speeds) in the future and as such conservative estimates are in order. Assuming ξ to be zero (for the Gumbel model) all the time automatically eliminates the uncertainty in the rate of tail decay which is a major component in extreme value modeling. The tendency of ξ for a specific station depends on the data itself and hence we think it is important that we do not make an apriori judgment

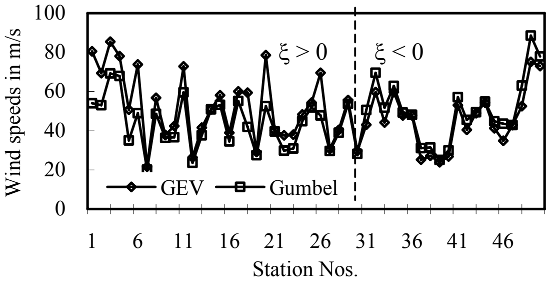

Fig. 15 Comparison of 50-year return wind speeds for GEV and Gumbel models for all stations

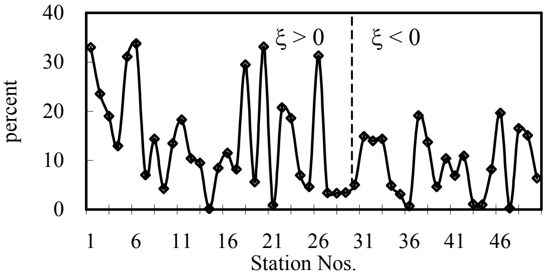

Fig. 16 Percent difference of 50-year return wind speeds between GEV and Gumbel models

about its value. For each station we let the "data speak for itself" regarding which extreme value model type it belongs and thus the GEV model is more appropriate for this purpose. In view of this it is preferable therefore to use the GEV model over the Gumbel model because it realistically considers the uncertainties inherent in the model extrapolation through ξ. Moreover acceptance of this uncertainty results in conservative estimates of return wind speeds.

An immediate consequence of this choice is the difference in the 50-year return wind speeds in both models (see **Fig. 15**). We can see that the extrapolated wind speeds for the GEV model are high compared to the Gumbel model when $\xi > 0$ and lower when $\xi < 0$. These differences are clearer if we take the percentage difference in the estimates of the GEV and Gumbel for each station as shown in **Fig. 16**. We can see that the GEV model improves the estimates by as much as 34% when $\xi > 0$ and as much as 20% when $\xi < 0$. Thus we conclude that the GEV is better over the Gumbel model as it serves our purpose in estimating conservative return wind speeds for design purposes.

In the succeeding section, we further improve the inference by using more extreme wind data, e.g. daily wind data, rather than just the annual maxima. Extreme events are scarce and therefore all available data should be utilized to improve the inference and to reduce the variance in the model estimates especially in return level approximations.

(3) The Point Process approach[8)]

The main weakness of the previous model is that the inference considers only one observation per year. Thus it is less flexible than threshold methods, e.g. generalized Pareto distribution (GPD) or r-largest order statistics model, where other extreme data are used into the inference. An alternative method in modeling extreme value behaviour that encompasses both the GEV and threshold methods is the point process model.

Let $X_1,..., X_n$ be a sequence of independent random variable with a common distribution function F. In our paper we assume that the daily maximum wind data are independent. Then characterizing the extremes according to Eq. (1), the distribution $M_n = \max(X_1,..., X_n)$ is GEV with parameters μ, σ and ξ for large n, with end points z_- and z_+.

Then for a suitably high threshold $u > z_-$, the sequence $X_1,..., X_n$ viewed on the interval (u, z_+) follow a non-homogeneous Poisson process with intensity measure on (u, z_+) as

$$\Lambda(u, z_+) = (1 + \xi(u - \mu)/\sigma)^{-1/\xi} \qquad (6)$$

To estimate the parameters of Eq. (6) we likewise use the ML method. Standard errors and approximate confidence intervals of the parameters are also estimated . The extreme quantiles or return wind speeds are obtained using the equation below:

$$x_N = \mu + \{(\sigma + \xi(u - \mu))/\xi\}[(Nn_y\zeta_u)^{\xi} - 1] \quad (7)$$

where N is the number of years, n_y is the number of observations per year while μ, σ and ξ are the point process model parameters. Also ζ_u is the probability of an individual observation exceeding the threshold u and is estimated by the following equation:

$$\hat{\zeta}_u = n_u / n \qquad (8)$$

where n_u is the number of observations exceeding the threshold u and n the total number of observations.

(4) Modeling daily maximum wind data

To apply the point process approach, a time series of daily maximum wind speeds (1961 to 2000) from Laoag City station is analyzed using the S-PLUS functions[9)]. The first step in the inference

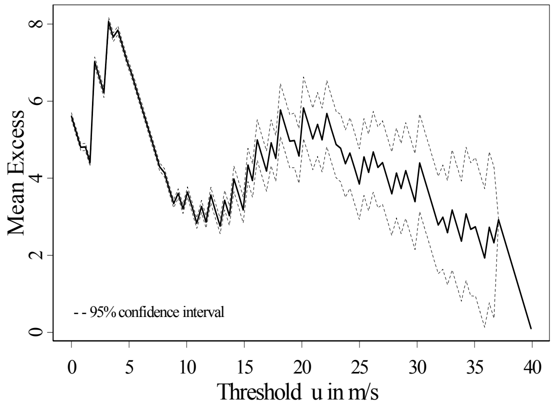

Fig. 17 Mean Residual Life Plot of Laoag Station data

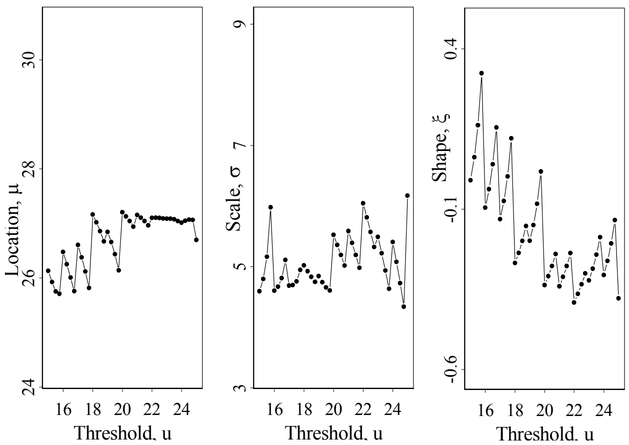

Fig. 18 MLEs of point process parameters vs. threshold

is to choose an appropriate threshold. As an aid, we will utilize two available methods.

The first, is the mean residual life plot developed by Davison and Smith[10] for the GPD. This is a plot of the sample mean of exceedances of the threshold u, against u. This plot tends to be linear if the GPD fits the data well. Since there is a direct connection between the GPD and the point process model we can make use of this tool.

The second method is to fit the point process model at a range of thresholds. At thresholds where the asymptotic argument is valid, stability in the parameter estimates might be observed. Although threshold choice is subjective, diagnostics e.g. quantile and probability plots help in checking the quality of the point process model fit. Also too low a threshold nullifies the asymptotic argument and a very high threshold gives few exceedances leading to high variance.

To illustrate this procedure, we show the mean residual life plot of the wind data from Laoag City station in **Fig. 17**. We can see that the plot is linear from $4 \leq u \leq 9$ but the thresholds are too low. On the other hand, the plot from $10 \leq u \leq 20$ shows a piece-

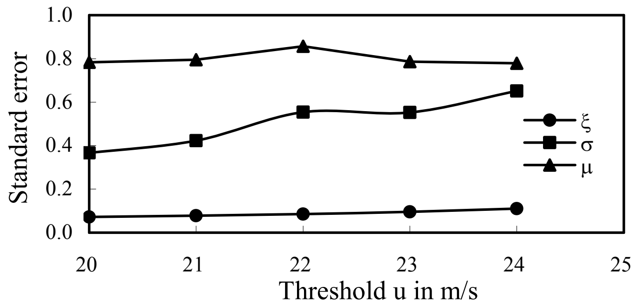

Fig. 19 Threshold u vs. parameter standard errors

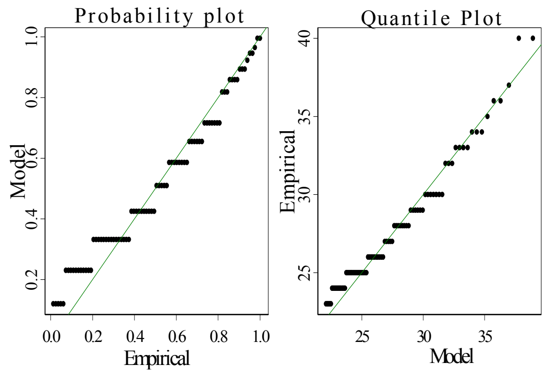

Fig. 20 Point Process diagnostic plots of Laoag Station data

wise linearity with a narrow 95% confidence interval. The threshold choice is not yet clear, so we look for support by examining the plot of the second method.

We show in **Fig. 18** a plot of the MLEs of the point process model against a range of threshold. In this figure, we can see that there seems to be a stability in the location parameter μ, at $u > 20$. Therefore using this range as a guide, the data is fitted to the point process model with thresholds ranging from $20 \leq u \leq 24$. **Fig. 19** shows the standard errors in the parameter estimates for each threshold. We note especially that the standard error for parameter ξ does not increase significantly as the threshold increases from 20 to 24.

Diagnostic plots of the point process model to the excess values for each threshold were also examined to determine the quality of the fit. Standard tools used in statistical analysis are the probability plot and the quantile plots[8].

The point process model $\hat{F}$ is an acceptable model for the data if the points of both the probability plot and the quantile plot are close to the unit line. Significant deviations from the line is an indication that $\hat{F}$ is a weak model for the data. More importantly we also examined if the data does not significantly depart (within the 95% CI) from the return wind plot. The return wind plots are similar to

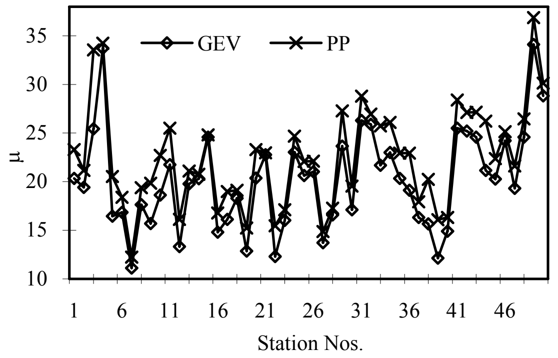

Fig. 21 Parameter μ for GEV and point process

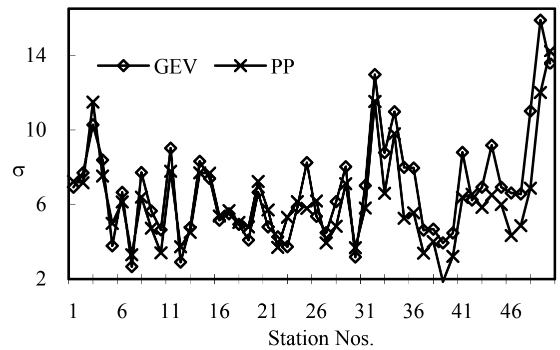

Fig .22 Parameter σ for GEV and point process

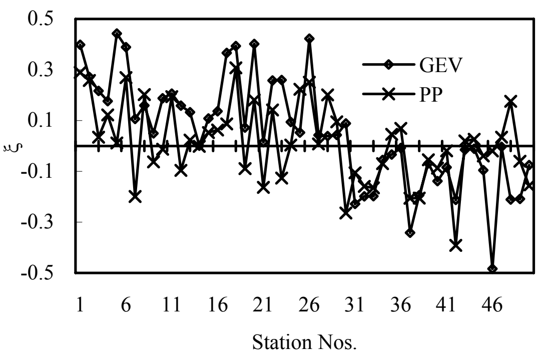

Fig. 23 Parameter ξ for GEV and point process

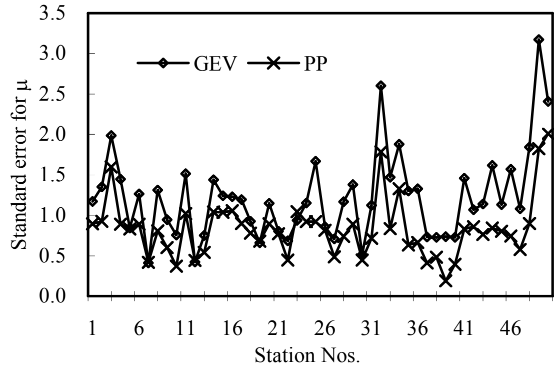

Fig. 24 Standard errors of μ for GEV and point process

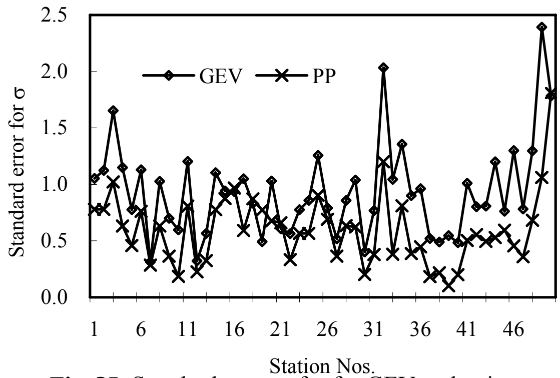

Fig. 25 Standard errors of σ for GEV and point process

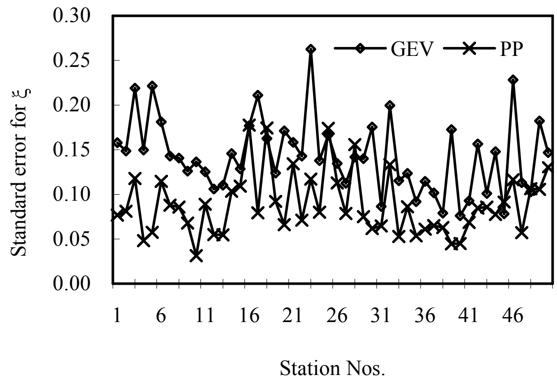

Fig .26 Standard error of ξ for GEV and point process

the GEV return wind plots shown in **Figs. 7, 8, 9** and **10**.

For the Laoag City station data, the diagnostic plots show that a threshold value $u = 22$ produces a better fit over the other threshold values as shown in **Fig. 20**. Therefore this threshold value with 83 exceedances shall be used in the point process model.

The resulting MLEs of the parameters are (27.10, 6.05, -0.39) with a maximized nllh of 246. The standard errors of the parameters are (0.86, 0.55, 0.08). Since there are 14,610 observations, ζ_u is equal to 83/14,610 = 0.01. Subsequently, the 50-year wind speed is calculated as 39 m/s. Subsequently, we apply the point process approach to the rest of the data sets to determine the MLEs of the parameters μ, σ and ξ for each station. The results of the point process approach fitting are shown in **Figs. 21**, **22** and **23**. Included in these plots are the results of the GEV model fit for comparison. The figures above show that there are marked differences in the MLEs of the parameters μ, σ and especially for ξ for each station. To assess the suitability of using the point process approach as an extreme value model for each station versus the GEV model, we compare the standard errors (standard deviation) in the MLEs of the parameters.

We can see in **Figs. 24**, **25** and **26** the reduction in the standard errors of the parameter estimates especially for ξ in the point process approach. This is the advantage of using more extreme data (greater

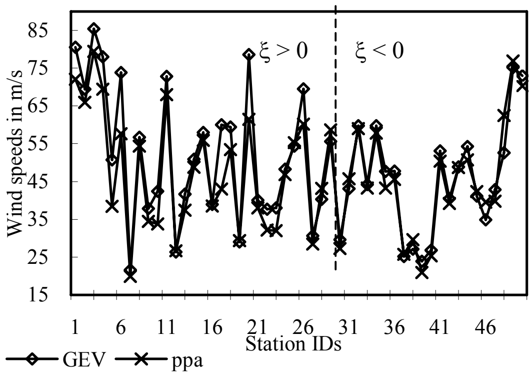

Fig .27 Comparison of 50-year return wind speeds for point process and GEV models for all stations

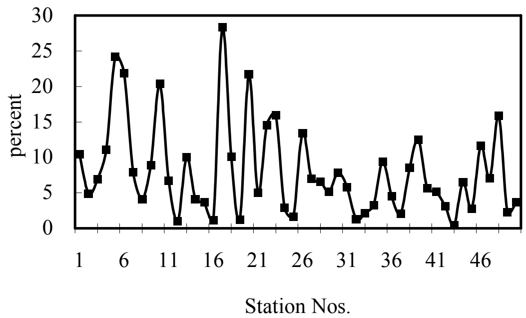

Fig. 28 Percent difference of 50-year return wind speeds between Point Process and GEV models

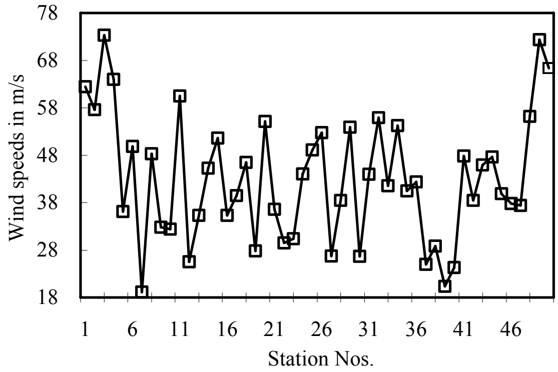

Fig. 29 30-year return wind speeds for point process

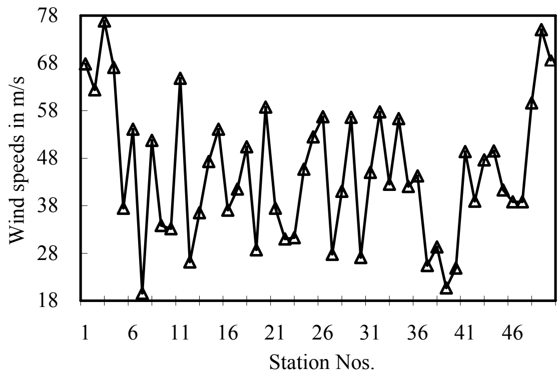

Fig .30 40-year return wind speeds for point process

than a specified threshold) than just annual maxima in the inference. This means that the point process approach is likely to more accurate than the GEV model fit. Therefore based on these results, we conclude that the point process is the most suitable model for characterizing extreme wind speeds in the Philippines. Suitable in the sense that it also accepts the uncertainty in the rate of the tail decay unlike the Gumbel model and better than the GEV because it considers other extreme data other than the annual maxima in the analysis.

The goodness-of-fit of the excess values with the point process model for each station was also assessed and we observed that the quality of fit for most stations were acceptable.

Again the immediate consequence of choosing the point process over the GEV and Gumbel model is the difference in 50-year return wind speeds. We can see from **Fig. 27** that wind speeds are lower in the point process than the GEV model for most station. The maximum percentage difference in the estimates is about 28% and the average is about 8% (see **Fig. 28**). We also compared percentage difference of the point process over the Gumbel model estimate and found that the former improves the estimates by as much as 25% when $\xi > 0$ and as much as 17% when $\xi < 0$.

Therefore these results shall be used in developing regional wind zone maps of extreme wind speeds for the Philippines. Aside from developing a wind zone map with an annual exceedance probability of 0.02 wind zone maps with annual exceedance probabilities of 0.033 (30-year return period) and 0.025 (40-year return period) were also developed. The motivation for this is that since available data are less than 40 years therefore extrapolation to lower return periods are more practical. The 30 and 40 year return wind speeds are shown in **Fig. 29** and **30**.

4. REGIONAL WIND ZONE MAP

Kriging is an interpolation method that predicts values at unmeasured locations using measured values from other locations. The weights used in this method come from a semivariogram calculated from the spatial structure of the data.

Assuming our data is stationary and normally distributed we can use kriging method to estimate the 50-year return wind speeds to other unmeasured areas using the results of point process model. We made several runs to create a prediction surface of the 50-year return wind speeds using kriging method of ArcGIS Geostatistical Analyst[11)]. The final result is the regional wind zone map with annual exceedance probability of 0.02 as shown in **Fig 31**.

The highlights of the proposed wind zone map are the following:

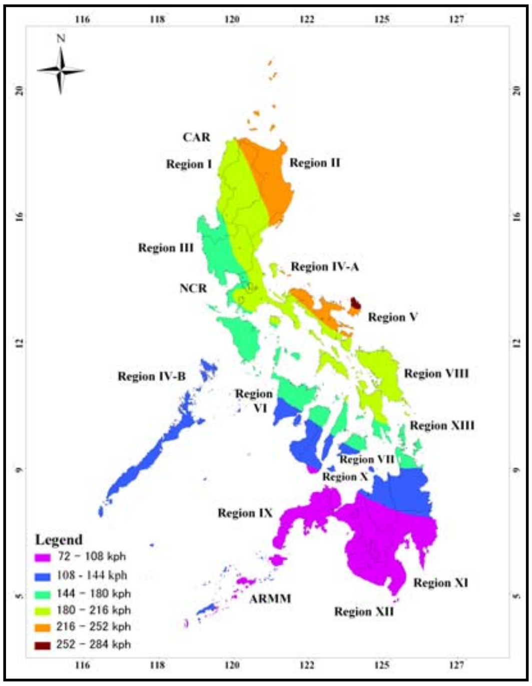

Fig. 31 Regional wind zone map for 50 year return wind speeds

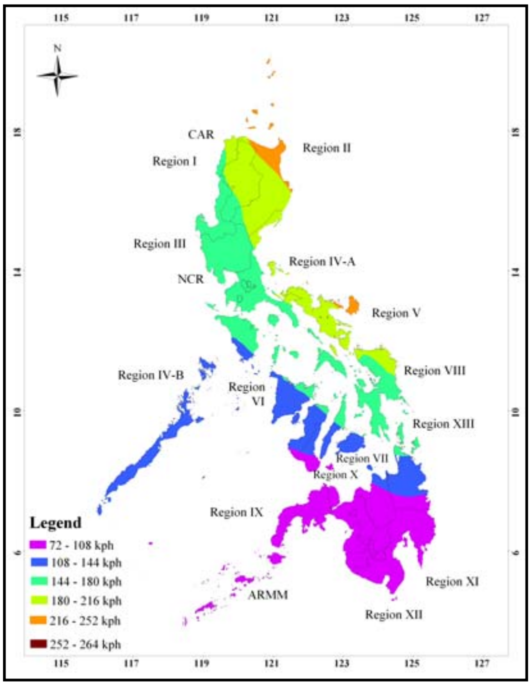

Fig. 32 Regional wind zone map for 30 year return wind speeds

1. Significant decrease in basic wind speeds for all zones of the recent wind zone map, especially in Zones II and III.
2. Slight increase in basic wind speeds at the boundary of Zone I and II of the recent wind zone map.
3. Areas where the expected 50-year wind speeds are greater than 70 m/s are identified. This information is vital for wind power projects in the future.
4. Six zones instead of three zones for easy conversion from meters per second to kilometers per hour, since the increment for each zone is 10 m/s.
5. Kriging method used in mapping enabled us to assess spatial correlation of extreme wind speeds using a spherical semivariogram. It also allowed us to generate a continuous prediction surface which is better than the recent wind zone map.
6. Regional boundaries are also added for ease in using the map.

Regional wind zone maps with annual exceedance probabilities of 0.033 and 0.025 are also shown in **Figs. 32** and **33**. These figures show that the wind speeds are increasing in a northeast to southwest direction. All three maps also show that the highest wind speeds are in the areas of Region II and V.

5. CONCLUDING REMARKS

The present wind zone map was generally developed based on the type I (Gumbel) distribution.

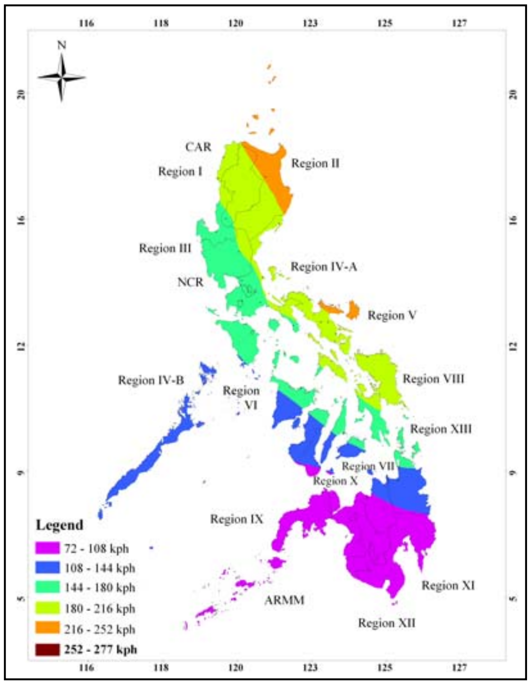

Fig. 33 Regional wind zone map for 40 year return wind speeds

Therefore we looked for alternatives in characterizing the extreme wind speeds in the Philippines using GEV distribution, Gumbel distribution and the point process approach. As a summary we show here the major works done and the conclusions arrived at in the study:

1. The extreme wind speed models for each station

was improved by taking advantage of the availability of recent and daily maximum wind data.
2. After fitting these extreme value models to the wind speed data, we can see that the point process model gives smaller standard errors in the parameter estimates making it a better model than GEV and Gumbel models.
3. A regional wind zone (6 zones) map of extreme wind speeds in the Philippines was developed from the results of the point process approach.

We also mention here that in our study we distinguished the regional boundaries and in our opinion is preferable over the previous zone maps because it follows regional / political boundaries and reduces misinterpretation in using the map.

ACKNOWLEDGMENT: The authors wish to thank PAGASA for providing wind data used in this research.

REFERENCES

1) Association of Structural Engineers of the Philippines: National Structural Code of the Philippines, Vol. 1, 5th Ed., 2001.
2) Coles, S. and Pericchi, L.: *Anticipating Catastrophes Through Extreme Value Modeling*, J. Roy. Stat. Soc., Ser. C, Vol. 52, pp. 405 – 416, 2003.
3) Ferreira, J. A. and Guedes Soares, C.: An Application of the Peaks Over Threshold Method to Predict Extremes of Significant Wave Height, *J. of Offshore Mechanics and Arctic Engineering*, Vol. 120, pp. 165 – 176, August 1998.
4) Smith, R. L.: Trends in Rainfall Extremes, Preprint, University of North Carolina, 1999.
5) Peterka, J. and Shahid, S.: Design Gust Wind Speeds in the United States, *J. of Structural Engineering*, Vol. 124, No. 2, pp. 207 – 214, February, 1998,
6) Mehta, K. C. and Marshall, R. D.: Guide to the use of the Wind Load Provisions of ASCE 7-95, ASCE Press, Virginia, USA, 1997.
7) Rosaria, N. E.: Estimation of Extreme Wind Speeds for the Development of Wind Zone Map for the Philippines, MS Thesis, University of the Philippines, Diliman, 2001.
8) Coles, S.: An Introduction to Statistical Modeling of Extreme Values, Springer-Verlag, 2001.
9) Coles, S.: *S-PLUS functions for extreme value modeling*, http://www.stats.bris.ac.uk/~masgc/ismev/functions.html.
10) Davison, A. and Smith, R.: *Models for exceedances over high thresholds* (with discussion), J. Roy. Statist. Soc., Ser B, Vol. 52, pp. 393 – 442, 1990.
11) Johnston, K., Ver Hoef, J. M. and Krivoruchko, K. and Lucas, N.: Using ArcGIS Geostatistical Analyst, ESRI 2001.

(Received April 19,2004)